Journal of Environmental Management 231 (2019): 726-733

**DOI:** https://doi.org/10.1016/j.jenvman.2018.10.031

# Anaerobic co-digestion of the aqueous phase from hydrothermally treated waste activated sludge with primary sewage sludge. A kinetic study

*John A. Villamil*, Angel F. Mohedano, Juan J. Rodriguez, M.A. De la Rubia*

Seccion de Ingenieria Quimica, Universidad Autonoma de Madrid, Madrid, Spain

*(john.villamil@uam.es)

**Abstract**

The mesophilic anaerobic co-digestion of the liquid fraction from hydrothermal carbonization (LFHTC) of dewatered waste activated sludge with primary sewage sludge (PSS) has been studied. Mixtures of different composition (25, 50 and 75% of LFHTC on a chemical oxygen demand (COD) basis), as well as the individual substrates, have been tested using two inocula (flocculent (FS) and granular (GS) sludges). Methane production decreased as the LFHTC/PSS ratio increased, which can be related to the presence of recalcitrant compounds in the LFHTC, such as alkenes, phenolics, and other oxygen- and nitrogen-bearing aromatics hard-to-degrade through anaerobic digestion. Methane yield reached 248 ± 11 mL CH4 STP/g CODadded with the GS inoculum and 25% LFHTC. A 74 and a 30% increase of methane production was achieved in the 25% LFHTC runs respect to the obtained in the similar experiments with 100% LFHTC, using the FS and GS inocula, respectively. In those late runs, the COD was reduced more than 86%, with a negligible concentration of total volatile fatty acids. With both inocula, total Kjeldahl nitrogen hydrolysis increased as the LFHTC to PSS mixture ratio decreased, reaching values higher than 79% at the end of the

experiments. Methane yield values fitted well the first-order, Cone and Weibull kinetic models for both inocula. Significant differences in the kinetic constant values, ranging from 0.100-0.168 $d^{-1}$ and 0.059-0.068 $d^{-1}$, were found with the FS and GS inocula, respectively. The results obtained support the potential integration of HTC of dewatered waste activated sludge in wastewater treatment plants.

**Keywords**

Anaerobic co-digestion (AcoD); biochemical methane potential (BMP); hydrothermal carbonization (HTC); sewage sludge; primary sewage sludge; kinetic model

## 1. Introduction

The management of sewage sludge (SS) plays a crucial role in wastewater treatment plants (WWTP). The huge generation of this biowaste could reach 13 Mt/year (on a dry basis) in 2020 in the European Union (Kelessidis and Stasinakis, 2012). Moreover, the high costs associated with SS treatment accounts for an essential part of total operational costs (Batstone et al., 2011). The conventional treatment of SS in large WWTP is mainly performed by anaerobic digestion. This technology allows recovering energy as biogas (≈36 $MJ/Nm^3$) in combined heat and power systems (cogeneration) and generators, to produce electricity and heat (Calise et al., 2015; Puyol et al., 2017, Wandera et al., 2018). However, anaerobic digestion suffers from some drawbacks such as the negative effect of biodegradable carbon and nutrient imbalance of the substrate on the biogas production. Optima carbon-to-nitrogen ratios (C/N) between 20 and 30 are commonly accepted for adequate anaerobic digestion. In this sense, SS is

characterized by a high organic matter content (60-70% on a dry basis), a relatively low C/N ratio, ranging between 6 and 16, and high buffer capacity, which affects to the nutrition balance of microorganisms (Silvestre et al., 2011). Therefore, the anaerobic co-digestion (AcoD) of sewage sludge with carbon-rich substrates with an adequate C/N ratio has been widely used for nutrients adjustment. These include the organic fraction of municipal solid wastes (OFMSW), food wastes, livestock and poultry manure and microalgae, among others (Mata-Alvarez et al., 2014, Nghiem et al., 2017; Nguyen et al., 2014; Thorin et al., 2018; Xie et al., 2017).

There are other technical solutions available for SS management such as incineration, composting and landfilling (Fijalkowski et al., 2017, Gutiérrez et al., 2017; Piippo et al., 2018). However, the emissions of greenhouse gases during incineration or the odor caused by composting process, make these solutions less attractive in many cases (Werther and Ogada, 1999). Several thermal processes for energy recovery, such as pyrolysis or gasification, are gaining attention, since the resultants products may be used as bio-fuels or source of chemicals (Alvarez et al., 2015; Manara and Zabaniotou, 2012). The main drawback of these technologies is the high energy requirements needed for moisture reduction.

In this context, hydrothermal carbonization (HTC) can be an environmentally friendly technology to manage SS allowing to reduce the energy-intensive drying of high-moisture organic feedstocks, as well as to produce the so-called hydrochar, a valuable solid fuel (Kumar et al., 2018). In this thermochemical process, wet biomass is treated within the range of 180 to 250 ºC and the corresponding equilibrium pressure (Funke and Ziegler, 2010; Libra et al., 2011). Different reactions such as hydrolysis,

dehydration, decarboxylation, condensation, and polymerization occur, yielding the abovementioned hydrochar, a gas stream (mainly $CO_2$) and a liquid fraction (LFHTC) containing volatile fatty acids (VFAs), furan compounds, glucose, phenols, pyrazines, pyrroles, among others (Danso-Boateng et al., 2015; De la Rubia et al., 2018a; Villamil et al., 2018a). Hydrochar from sewage sludge can be used as fuel due to its good higher heating value ((HHV) ≈ 19-24 MJ/kg), comparable to sub-bituminous coals (Danso-Boateng et al., 2015). Moreover, this carbon material can be applied in soil amendment, environmental remediation and as low-cost adsorbent (Gwenzi et al., 2017, Kim et al., 2014). The liquid by-product from SS carbonization is characterized by high organic matter and nitrogen contents (De la Rubia et al., 2018b; Posmanik et al., 2017; Villamil et al., 2018b) and must be treated to avoid adverse environmental impacts. Taking into account the presence of several compounds readily biodegradable (formic, acetic, iso-butyric and butyric acids), this fraction can be valorized as a substrate for anaerobic digestion (Luz et al., 2018; Qiao et al., 2011; Wirth and Mumme, 2013). The main drawback for that is its low C/N ratio (around 7) (Villamil et al., 2018a). Thus, AcoD with PSS can provide a potential solution which would allow the integration of waste activated sludge HTC in the scheme of sludge processing in WWTP with the benefit of producing hydrochar in addition to biogas. Fig. 1 shows a proposal of a flow diagram for this approach.

The aim of the current work is to evaluate this new concept for sewage sludge management. Mesophilic anaerobic co-digestion of mixtures of the LFHTC of dewatered waste activated sludge and thickened primary sewage sludge, as well as the two bare substrates (PSS and LFHTC), have been tested using two fairly different inocula (a

flocculent sludge from a mesophilic digester of a municipal wastewater treatment and a granular ones from a brewery wastewater treatment plant). Several key parameters (alkalinity, Total Kjeldahl nitrogen (TKN), total ammoniacal nitrogen (TAN), VFA, COD and methane yield) of anaerobic process were assessed upon digestion time. Finally, cumulate methane production was fitted to widely applied kinetic models (first order, Gompertz, modified Gompertz, Cone, and Weibull equations) in anaerobic digestion.

Waste activated sludge was selected for HTC experiments instead of a mixture of both primary (PSS) and sencondary sewage sludge, because of some advantages: (i) Improve the quality of the hydrochar since SS has lower ash content (usually around 20%) versus more than 30% of PSS and (ii) increase of the potential phosphorus recovery from the liquid fraction since secondary SS presents higher P content (McGaughy and Reza, 2018). In addition, it is well known that secondary SS shows poor digestibility compared to PSS.

## 2. MATERIALS AND METHODS

### *2.1. Inocula and substrates characterization*

Two different inocula were used: (i) An anaerobic flocculent sludge (FS inoculum) from a full-scale mesophilic digester treating mixed sewage sludge, and (ii) a granular inoculum obtained from a high rate anaerobic reactor, which treats brewery wastewater (GS inoculum). Table 1 depicts representative analysis of those inocula.

LFHTC was obtained from HTC of DSS (15% dry matter) was collected from a cosmetic factory full-scale membrane bioreactor (Madrid, Spain), frozen (-20 °C) and stored before use. HTC experiments were conducted in a 4 L stainless steel reactor

(ZipperClave). In each batch experiment, approximately 1.5 kg of the DSS was loaded into the vessel. The chosen temperature (208 ºC) was reached heating at 3 ºC/min and maintaining the carbonization time for 1 h. Once cooled, the liquid fraction was centrifuged and filtered (0.45 µm). PSS was drawn from the thickener of a WWTP (Madrid, Spain). Table 1 includes representative analysis of both substrates.

### *2.2. Batch anaerobic experiments*

AcoD experiments were performed in 120 mL glass digesters. Each flask contained a final concentration of 10 g COD/L inoculum, and different concentrations of PSS and LFHTC, together with a stock mineral medium solution and deionized water to make up the working volume (60 mL), following the indications provided by Holliger et al. (2016). Blank tests were performed with inoculum and mineral medium. Tests with starch as sole substrate were also carried out as positive controls. The vials were flushed with $N_2$ to get anaerobic conditions and placed in a shaking water bath at 35 ± 1 °C. An ISR of 2 on a COD basis (or 1.7 on a volatile solid (VS) basis) were selected as operational conditions. All the experiments were run until the accumulated gas production remained essentially unchanged, so that biodegradation could be considered essentially completed. Mixtures of different LFHTC to PSS ratios (on a COD basis) (25, 50 and 75% LFHTC), as well as the two bare substrates (LFHTC and PSS) were tested. These co-substrates are referred as 0LF, 25LF, 50LF, 75LF and 100LF. Nine glass serum vials were used for each experiment, sacrificing periodically samples one to six for characterization (after centrifuging and filtering them), and using the other three for biogas composition and volume determinations. Moreover, three blank tests with only

inoculum and three positive control tests with starch as the sole substrate were performed with each inoculum.

### *2.3. Analytical methods*

Elemental composition (C, H, N, S) content of DSS and hydrochar was determined using a LECO CHNS-932 Elemental Analyzer. ASTM methods D3173-11, D3174-11 and D3175-11, were used to determine the moisture, ash and volatile matter, respectively.

Total solids (TS), VS, soluble COD (SCOD) and TAN, were measured using standard methods (2540b, 2540d, 5220-d and 4500-$NH_3$ APHA, 1998, respectively) while free ammonia nitrogen (FAN) was calculated according to Hansen et al. (1998). pH was measured with a Crison Basic pH meter. Alkalinity was measured by titration with 0.02 N $H_2SO_4$ to endpoints of pH 5.75 and 4.3, allowing calculation of total (TA), partial (PA) and intermediate alkalinity (IA) (Ripley et al., 1986). Total COD (TCOD) was determined by the proposed method by Raposo et al. (2008). TKN was determined as it has been described elsewhere (Villamil et al., 2018a), total organic carbon (TOC) was measured with TOC-VCPN (Shimadzu) automatic analyzer. Volatile fatty acids (VFA) were quantified in a Varian 430-GC gas chromatograph (De la Rubia et al., 2018b). Chemical species were identified in a GC–MS CP-3800/Saturn 2200 using a Varian CP-8200 autosampler injector (De la Rubia et al., 2018b).

Biogas volume produced was measured by an electronic manometer (ifm, PN 7097) and expressed at standard pressure and temperature conditions (STP) (273 K, 1 bar). Gas composition ($H_2$, $H_2S$, $CO_2$ and $CH_4$) was analyzed by a Thermo Scientific Trace

1310 gas chromatography (De la Rubia et al., 2018b). Cumulative methane yield on the last day for FS and GS inocula, were assessed by analysis of variance (ANOVA) using Origin software (version 9.0). Fisher's least significant difference (Fisher's LSD) was calculated at a confidence level of 0.05.

## 3. RESULTS AND DISCUSSION

Fig. 2 shows the TKN values and the evolution of TAN upon the AcoD of the two substrates tested. As can be seen, the hydrolytic stage was shorter for the experiments with the FS inoculum (Fig. 2a) than for those with GS (Fig. 2b). TKN hydrolysis decreased at increasing the HTC percentage in the mixture, reaching similar final values (79-95%) for each mixture ratio with both inocula. Final TAN values were within the range of 600-800 and 460-650 mg N/L for the experiments with FS and GS, respectively, much lower than the considered inhibitory value for methanogenic microorganism (1700 mg N/L) (Franke-Whittle et al., 2014). The pH values (6.8-7.3) remained relatively constant in all the runs within the adequate range for methanogenic *Archaea* growing (Parameswaran and Rittmann, 2012).

Fig. 3 shows the evolution of alkalinity along the experiments. The initial TA ranged from 1.1 to 1.6 g/L $CaCO_3$ and showed a continuous increase along the anaerobic process, probably due to the release of carbon dioxide and ammonia nitrogen upon the decomposition of the organic matter with time, which improves the buffer capacity (Córdoba et al., 2016). Final TA values in the range of 2.4-2.8 g/L $CaCO_3$ were reached, providing enough buffer capacity (> 2 g/L $CaCO_3$) as has been recommended in the literature (Angenent et al., 2002; Cook et al., 2017).

Fig. 4 depicts the time-course of total VFA (TVFA) expressed as mg COD/L. The concentration of acetic, propionic and iso-valeric acids in the LFHTC of DSS, yielded values of 3532 ± 123 mg/L, 620 ± 10 mg/L and 78 ± 19 mg/L, respectively. In the FS experiments (Fig. 4a), values of COD attributable to VFA ranged from 455 to 805 mg COD/L in the first days. TVFA concentration decrease after the hydrolytic-acidogenic stage, reaching negligible values after 10 days digestion time. The TVFA concentrations in the GS experiments (Fig. 4b) were significantly higher than the obtained with FS in the first days, reaching values between 778 and 1284 mg COD/L, but then follows a similar trend. Therefore, no VFA were accumulated under the experimental conditions tested, which means that there was no imbalance in the anaerobic process with none of the inocula used.

Fig. 5 shows the evolution of SCOD upon digestion time. The initial SCOD values in all the experiments were around 5 g COD/L. Somewhat higher COD removal was achieved with the granular inoculum (78-95% vs. 70-87%). Similar SCOD removal (80%) for anaerobic batch reactor treating the LFHTC of digestate (220 ºC-30 min) has been reported (Aragón-Briceño et al., 2017). The COD attributable to VFA was less than 27% in the FS runs during the hydrolytic-acidogenic stage. In the GS experiments, the VFAs were consumed completely during that stage (first 10 days). The remaining COD corresponds to refractory compounds which were detected in the LFHTC of DSS such as heterocyclic organic species (pyrroles, pyridines), ketones and alcohols (De la Rubia et al., 2018a; Villamil et al., 2018a), inhibiting methanogenesis, mainly in the case of aromatics (Chen et al., 2008). It can also be ascribable to pyrazine compounds which are Maillard products generated in HTC reactions between reducing sugars and amino

acids (Titirici, 2013). Moreover, the presence of several nitrogen-containing aromatic compounds could be related to the high TKN concentration in the liquid phase.

Fig. 6 shows the cumulative methane production along the anaerobic digestion experiments. Final values ranged within 98 ± 3-204 ± 1 and 191 ± 1-308 ± 1 mL $CH_4$ STP/g $COD_{added}$ for FS and GS experiments, respectively. Several authors have also observed higher methane yields with granular inocula than with the flocculent ones due to the abundance and diversity of methanogenic microorganisms in the granules (De la Rubia et al., 2018b; De Vrieze et al., 2015; Neves et al., 2004; Rincon et al., 2011). With both inocula, the methane production increased at decreasing the LFHTC to PSS ratio mixture. In this way, for FS inoculum, a 1.30-fold increase in methane yield was achieved for 25LF experiment compared to the experiment performed with LFHTC as mono-substrate (100LF), while for GS a 1.74-fold increase was reached.

The yield obtained with the FS inoculum in the 25LF experiment (172 ± 1 mL $CH_4$ STP/g $COD_{added}$) was similar to the reported by Wirth et al. (2015) (120-180 mL $CH_4$ STP/g $COD_{added}$) for the continuous anaerobic digestion of LFHTC of digested sewage sludge. Qiao et al. (2011) reported a methane yield of 257 mL $CH_4$/g COD operating a continuous UASB reactor, while Aragón-Briceño et al. (2017) found values up to 277 mL $CH_4$ STP/g $COD_{added}$ for batch operation, both of them fed with LFHTC of digested sewage sludge. This yield is similar to the obtained in the current work from the 25LF mixture with GS inoculum (248 ± 11 mL $CH_4$ STP/g $COD_{added}$). Recently, De la Rubia et al. (2018a) have studied the mesophilic co-digestion of the LFHTC of secondary SS and OFMSW using a flocculent inoculum, reaching an ultimate methane yield within the range of 124 ± 9 and 194 ± 1 mL $CH_4$ STP/g $COD_{added}$, very close to the obtained now

with the FS inoculum. Several studies can be found in the literature dealing with anaerobic digestion of the LFHTC of several biomass wastes. The ultimate methane yield depends on nature of the raw residue and the HTC conditions (time and temperature). Close values to the obtained in the 25LF experiments of this study (175-300 mL $CH_4$/g COD) have been reported with the LFHTC of lignocellulosic residues (Erdogan et al., 2015, Weiner et al., 2016, Wood et al., 2013).

Fig. 7 shows the daily methane production rate, calculated as the derivative of the cumulative methane yield. As can be seen, with the FS inoculum the methane production rate decreased at increasing the relative amount of LFHTC in the mixture. The highest values (12.7-33.3 mL $CH_4$/g COD d) were reached in the $2^{nd}$ day, corresponding with the VFA concentration peak. Lower values (11.1-21.3 mL $CH_4$/g COD d) were obtained with the GS inoculum, probably due to mass-transfer limitation of VFA in this granular sludge (Gonzalez-Gil et al., 2001).

The results of methane yield were fitted to first-order, Gompertz, modified Gompertz, Cone and Weibull kinetic models, which have been widely applied for anaerobic digestion (El-Mashad, 2013; Nielfa et al., 2015; Ragaglini et al., 2014; Raposo et al., 2011; Zhao et al., 2016). Table 3 collects the above-mentioned kinetic equations. Origin software (version 8.0) was used to fit the experimental data to those kinetic equations. The results are summarized in Tables 4 (FS experiments) and 5 (GS experiments).

Except for modified Gompertz model, all the kinetic equation checked describe well the evolution of methane production upon digestion time. In general, the fitting was better for the experiments with the flocculent inoculum (FS). The *k* values obtained for first-order apparent rate constant fall within the range of 0.100-0.168 $d^{-1}$ and 0.059-0.068 $d^{-1}$

for FS and GS experiments, respectively. The lower *k* values with the granular sludge can be due to the occurrence of mass-transport limitation (Gonzalez-Gil et al., 2001). All the *k* values are higher than the reported by Villamil et al. (2018a) for the anaerobic digestion of the LFHTC of DSS (0.031-0.043 $d^{-1}$) but significantly lower than the previously reported by De la Rubia et al. (2018a) for the AcoD of the OFMSW with the LFHTC of waste activated sludge (0.44-0.56 $d^{-1}$).

## 4. CONCLUSIONS

The co-digestion of LFHTC and PSS can provide a feasible way of integrating the HTC of waste activated sludge in a WWTP. Increasing the LFHTC to PSS ratio decreases the methane production, due to the presence of inhibitory nitrogen-containing aromatic compounds detected in the LFHTC. The granular inoculum (GS) was better in terms of ultimate methane yield than the flocculent one (FS). The highest methane yields were found for the experiments with 25% LFHTC (1.76 and 1.30-fold increase with respect to the bare LFHTC, with FS and GS inocula, respectively). With that mixture, SCOD removals around 85-90% were obtained, with no residual VFAs detected. Further research will be required to evaluate the co-digestion of LFHTC and PSS in semi-continuous experiments and with LFHTC below 25% in the mixture.

## ACKNOWLEDGEMENTS

The authors greatly appreciate financial support from the Spanish MINECO (Project CTM2016-76564-R) and the Community of Madrid (Project P2013/MAE-2716). M.A. de la Rubia acknowledges financial support from the Spanish Ministry of Economy and

Competitiveness (RYC-2013-12549). The valuable contribution of N. Ocaña is also acknowledged.

## REFERENCES

Aragón-Briceño, C., Ross, A.B., Camargo-Valero, M.A., 2017. Evaluation and comparison of product yields and bio-methane potential in sewage digestate following hydrothermal treatment. Appl. Energy 208, 1357–1369.

Alvarez, J., Amutio, M., Lopez, G., Barbarias, I., Bilbao, J., Olazar, M., 2015. Sewage sludge valorization by flash pyrolysis in a conical spouted bed reactor. Chem. Eng. J. 273, 173–183.

Angenent, L.T., Sung, S., Raskin, L., 2002. Methanogenic population dynamics during startup of a full-scale anaerobic sequencing batch reactor treating swine waste. Water Res. 36, 4648–4654.

APHA, 1998. Standard Methods for the Examination of Water and Wastewater, 20th edn, American Public Health Association, American Water Works Association and Water Environment Federation. Washington DC.

Batstone, D.J., Jensen, P.D., Ge, H., 2011. Biochemical treatment of biosolids-emerging technologies. Water 5, 90–93.

Calise, F., Cremonesi, C., de Notaristefani di Vastogirardi, G., D'Accadia, M.D., 2015. Technical and economic analysis of a cogeneration plant fueled by biogas produced from livestock biomass. Energy Procedia 82, 666–673.

Chen, Y., Cheng, J.J., Creamer, K.S., 2008. Inhibition of anaerobic digestion process: A review. Bioresour. Technol. 99, 4044–4064.

Cook, S.M., Skerlos, S.J., Raskin, L., Love, N.G., 2017. A stability assessment tool for anaerobic codigestion. Water Res. 112, 19–28.

Córdoba, V., Fernández, M., Santalla, E., 2016. The effect of different inoculums on anaerobic digestion of swine wastewater. J. Environ. Chem. Eng. 4, 115–122.

Danso-Boateng, E., Shama, G., Wheatley, A.D., Martin, S.J., Holdich, R.G., 2015. Hydrothermal carbonisation of sewage sludge: effect of process conditions on product characteristics and methane production. Bioresour. Technol. 177, 318–27.

De la Rubia, M.A., Villamil, J.A., Rodriguez, J.J., Borja, R., Mohedano, A.F., 2018a. Mesophilic anaerobic co-digestion of the organic fraction of municipal solid waste with the liquid fraction from hydrothermal carbonization of sewage sludge. Waste Manage. doi:https://doi.org/10.1016/j.wasman.2018.02.046.

De la Rubia, M.A., Villamil, J.A., Rodriguez, J.J., Mohedano, A.F., 2018b. Effect of inoculum source and initial concentration on the anaerobic digestion of the liquid fraction from hydrothermal carbonisation of sewage sludge. Renew. Energy. 127, 697-704.

De Vrieze, J., Raport, L., Willems, B., Verbrugge, S., Volcke, E., Meers, E., Angenent, L.T., Boon, N. 2015. Inoculum selection influences the biochemical methane potential of agro-industrial substrates. Microbial Biotechnol. 8, 776–786.

El-Mashad, H.M., 2013. Kinetics of methane production from the codigestion of switchgrass and *Spirulina platensis* algae. Bioresour. Technol. 132, 305–312.

Erdogan, E., Atila, B., Mumme, J., Reza, M.T., Toptas, A., Elibol, M., Yanik, J., 2015. Characterization of products from hydrothermal carbonization of orange pomace including anaerobic digestibility of process liquor. Bioresour. Technol. 196, 35–42.

Fijalkowski, K., Rorat, A., Grobelak, A., Kacprzak, M.J., 2017. The presence of contaminations in sewage sludge – The current situation. J. Environ. Manage. 203, 1126–1136

Franke-Whittle, I.H., Walter, A., Ebner, C., Insam, H., 2014. Investigation into the effect of high concentrations of volatile fatty acids in anaerobic digestion on methanogenic communities. Waste Manage. 34, 2080–2089.

Funke, A., Ziegler, F., 2010. Hydrothermal carbonization of biomass: A summary and discussion of chemical mechanisms for process engineering. Biofuels, Bioprod. Biorefining 4, 160–177.

Gonzalez-Gil, G., Seghezzo, L., Lettinga, G., Kleerebezem, R., 2001. Kinetics and mass-transfer phenomena in anaerobic granular sludge. Biotechnol. Bioeng. 73, 125–134.

Gutiérrez, M.C., Serrano, A., Siles, J.A., Chica, A.F., Martín, M.A., 2017. Centralized management of sewage sludge and agro-industrial waste through co-composting. J. Environ. Manage. 196, 387–393.

Gwenzi, W., Chaukura, N., Noubactep, C., Mukome, F.N.D., 2017. Biochar-based water treatment systems as a potential low-cost and sustainable technology for clean water provision. J. Environ. Manage. 197, 732–749.

Holliger, C., Alves, M., Andrade, D., [...], van Lier, J., Wedwitschka, H., Wierinck, I., 2016. Towards a standardization of biomethane potential tests. Water Sci. Technol. 74, 2515-2522.

Kelessidis, A., Stasinakis, A.S., 2012. Comparative study of the methods used for treatment and final disposal of sewage sludge in European countries. Waste

Manage. 32, 1186–1195.

Kim, D., Lee, K., Park, K.Y., 2014. Hydrothermal carbonization of anaerobically digested sludge for solid fuel production and energy recovery. Fuel 130, 120–125.

Kumar, M., Olajire Oyedun, A., Kumar, A., 2018. A review on the current status of various hydrothermal technologies on biomass feedstock. Renew. Sustain. Energy Rev. 81, 1742–1770.

Libra, J.A., Ro, K.S., Kammann, C., Funke, A., Berge, N.D., Neubauer, Y., Titirici, M.-M., Fühner, C., Bens, O., Kern, J., Emmerich, K.-H., 2011. Hydrothermal carbonization of biomass residuals: a comparative review of the chemistry, processes and applications of wet and dry pyrolysis. Biofuels 2, 71–106.

Luz, F.C., Volpe, M., Fiori, L., Manni, A., Cordiner, S., Mulone, V., Rocco, V., 2018. Spent coffee enhanced biomethane potential via an integrated hydrothermal carbonization-anaerobic digestion process. Bioresour. Technol. doi:https://doi.org/10.1016/j.biortech.2018.02.021

Mata-Alvarez, J., Dosta, J., Romero-Güiza, M.S., Fonoll, X., Peces, M., Astals, S., 2014. A critical review on anaerobic co-digestion achievements between 2010 and 2013. Renew. Sustain. Energy Rev. 36, 412–427.

Manara, P., Zabaniotou, A., 2012. Towards sewage sludge based biofuels via thermochemical conversion – A review. Renew. Sustain. Energy Rev. 16, 2566–2582.

McGaughy, K., Reza, M.T., 2018. Recovery of macro and micro-nutrients by hydrothermal carbonization of septage. J. Agric. Food Chem. 66, 1854–1862.

Neves, L., Oliveira, R., Alves, M.M. 2004. Influence of inoculum activity on the

biomethanization of a kitchen waste under different waste/inoculum ratios. Process Biochem. 39, 2019–2024.

Nghiem, L.D., Koch, K., Bolzonella, D., Drewes, J.E., 2017. Full scale co-digestion of wastewater sludge and food waste: Bottlenecks and possibilities. Renew. Sustain. Energy Rev. 72, 354–362.

Nguyen, L.N., Hai, F.I., Nghiem, L.D., Kang, J., Price, W.E., Park, C., Yamamoto, K., 2014. Enhancement of removal of trace organic contaminants by powdered activated carbon dosing into membrane bioreactors. J. Taiwan Inst. Chem. Eng. 45, 571–578.

Nielfa, A., Cano, R., Vinot, M., Fernández, E., Fdz-Polanco, M., 2015. Anaerobic digestion modeling of the main components of organic fraction of municipal solid waste. Process Saf. Environ. Prot. 94, 180–187.

Parameswaran, P., Rittmann, B.E., 2012. Feasibility of anaerobic co-digestion of pig waste and paper sludge. Bioresour. Technol. 124, 163–168.

Piippo, S., Lauronen, M., Postila, H., 2018. Greenhouse gas emissions from different sewage sludge treatment methods in north. J. Clean. Prod. 177, 483–492.

Posmanik, R., Labatut, R.A., Kim, A.H., Usack, J.G., Tester, J.W., Angenent, L.T., 2017. Coupling hydrothermal liquefaction and anaerobic digestion for energy valorization from model biomass feedstocks. Bioresour. Technol. 233, 134–143.

Puyol, D., Batstone, D.J., Hülsen, T., Astals, S., Peces, M., Krömer, J.O., 2017. Resource Recovery from Wastewater by Biological Technologies: Opportunities, Challenges, and Prospects. Front. Microbiol. 7, 1-23.

Qiao, W., Peng, C., Wang, W., Zhang, Z., 2011. Biogas production from supernatant of

hydrothermally treated municipal sludge by upflow anaerobic sludge blanket reactor. Bioresour. Technol. 102, 9904–9911.

Ragaglini, G., Dragoni, F., Simone, M., Bonari, E., 2014. Suitability of giant reed (*Arundo donax L.*) for anaerobic digestion: Effect of harvest time and frequency on the biomethane yield potential. Bioresour. Technol. 152, 107–115.

Raposo, F., de la Rubia, M.A., Borja, R., Alaiz, M., 2008. Assessment of a modified and optimised method for determining chemical oxygen demand of solid substrates and solutions with high suspended solid content. Talanta 76, 448–453.

Raposo, F., Fernández-Cegrí, V., De la Rubia, M.A. [...], Wierinck, I., Wilde, V., 2011. Biochemical methane potential (BMP) of solid organic substrates: Evaluation of anaerobic biodegradability using data from an international interlaboratory study. J. Chem. Technol. Biotechnol. 86, 1088–1098.

Rincón, B., Portillo, M.C., González, J.M., Fernández-Cegrí, V., De la Rubia, M.A., Borja, R. 2011. Feasibility of sunflower oil cake degradation with three different anaerobic consortia. J. Environ. Sci. Health. Part A 46, 1409-1416.

Silvestre, G., Rodríguez-Abalde, A., Fernández, B., Flotats, X., Bonmatí, A., 2011. Biomass adaptation over anaerobic co-digestion of sewage sludge and trapped grease waste. Bioresour. Technol. 102, 6830–6836.

Thorin, E., Olsson, J., Schwede, S., Nehrenheim, E., 2018. Co-digestion of sewage sludge and microalgae – Biogas production investigations. Appl. Energy. doi: https://doi.org/10.1016/j.apenergy.2017.08.085

Titirici, M.M., 2013. Hydrothermal Carbonisation: A Sustainable Alternative to Versatile Carbon Materials. Habilitation Thesis, Universität Potsdam, Potsdam.

Villamil, J.A., Mohedano, A.F., Rodriguez, J.J., de la Rubia, M.A., 2018a. Valorisation of the liquid fraction from hydrothermal carbonisation of sewage sludge by anaerobic digestion. J. Chem. Technol. Biotechnol. 93, 450-456.

Villamil, J.A., Mohedano A.F., Rodriguez J.J., Borja R., De la Rubia M.A., 2018b Anaerobic co-digestion of the Organic Fraction of Municipal Solid Waste and the Liquid Fraction From the Hydrothermal Carbonization of Industrial Sewage Sludge Under Thermophilic Conditions. Front. Sustain. Food Syst. 2:17. doi: https://doi.org/10.3389/fsufs.2018.00017

Wandera, S.M., Qiao, W., Algapani, D.E., Bi, S., Yin, D., Qi, X., Liu, Y., Dach, J., Dong, R., 2018. Searching for possibilities to improve the performance of full scale agricultural biogas plants. Renew. Energy 116, 720–727.

Weiner, B., Wedwitschka, H., Poerschmann, J., Kopinke, F.-D., 2016. Utilization of Organosolv Waste Waters as Liquid Phase for Hydrothermal Carbonization of Chaff. ACS Sustain. Chem. Eng. 4, 5737–5742.

Werther, J., Ogada, T., 1999. Sewage sludge combustion. Prog. Energy Combust. Sci. 25, 55–116.

Wirth, B., Mumme, J., 2013. Anaerobic digestion of waste water from hydrothermal carbonization of corn silage. Appl. Bioenergy 1, 1–10.

Wirth, B., Reza, T., Mumme, J., 2015. Influence of digestion temperature and organic loading rate on the continuous anaerobic treatment of process liquor from hydrothermal carbonization of sewage sludge. Bioresour. Technol. 198, 215–222.

Wood, B.M., Jader, L.R., Schendel, F.J., Hahn, N.J., Valentas, K.J., Mcnamara, P.J., Novak, P. M., Heilmann, S.M., 2013. Industrial symbiosis: Corn ethanol

fermentation, hydrothermal carbonization, and anaerobic digestion. Biotechnol. Bioeng. 110, 2624–2632.

Xie, S., Wickham, R., Nghiem, L.D., 2017. Synergistic effect from anaerobic co-digestion of sewage sludge and organic wastes. Int. Biodeterior. Biodegrad. 116, 191–197.

Zhao, C., Yan, H., Liu, Y., Huang, Y., Zhang, R., Chen, C., Liu, G., 2016. Bio-energy conversion performance, biodegradability, and kinetic analysis of different fruit residues during discontinuous anaerobic digestion. Waste Manage. 52, 295–301.

Table 1. Representative analysis[a] of the inocula (FS and GS) and substrates (PSS and LFHTC).

| | Inoculum | | Substrate | |
|---|---|---|---|---|
| | **FS** | **GS** | **PSS** | **LFHTC** |
| pH | 6.9 ± 0.1 | 7.2 ± 0.2 | 5.1 ± 0.1 | 4.9 ± 0.2 |
| TS (g/kg) | 21.1 ± 0.1 | 46.1 ± 0.7 | 53.1 ± 0.1 | 51.9 ± 0.5 |
| VS (g/kg) | 13.9 ± 0.3 | 40.3 ± 0.1 | 45.7 ± 0.1 | 24.0 ± 0.5 |
| TCOD (g $O_2$/L) | 24.8 ± 0.8 | 91.2 ± 1.4 | 78.9 ± 4.2 | 110.1 ± 2.3 |
| TKN (g N/L) | 3.9 ± 0.2 | 5.1 ± 0.1 | 3.8 ± 0.3 | 8.4 ± 0.6 |
| Na (mg/g) | 3.0 ± 0.1 | 0.8 ± 0.1 | 3.1 ± 0.1 | 1074.0 ± 11.6 |
| Mg (mg/g) | 3.7 ± 0.1 | 0.1 ± 0.0 | 3.8 ± 0.2 | 23.2 ± 1.3 |
| Al (mg/g) | 8.9 ± 0.1 | 0.6 ± 0.0 | 9.5 ± 0.4 | 15.8 ± 0.7 |
| K (mg/g) | 4.7 ± 0.1 | 0.5 ± 0.1 | 4.9 ± 0.8 | 1182.7 ± 66.1 |
| Ca (mg/g) | 39.2 ± 1.4 | 0.3 ± 0.1 | 33.0 ± 0.3 | 67.5 ± 4.4 |
| Fe (mg/g) | 24.8 ± 0.5 | < 0.1 | 28.5 ± 0.5 | 32.5 ± 0.1 |

[a] Average values of three determinations with standard deviations.

Table 2. Representative analysis[a] of the dewatered secondary sludge and the resulting hydrochar (% d.b.).

| | Waste activated sludge | Hydrochar |
|---|---|---|
| C | 41.5 ± 0.1 | 43.1 ± 0.2 |
| H | 6.0 ± 0.1 | 5.8 ± 0.1 |
| N | 6.8 ± 0.2 | 4.6 ± 0.1 |
| S | 0.7 ± 0.1 | 0.2 ± 0.1 |
| O[b] | 31.3 ± 0.2 | 26.5 ± 0.1 |
| Ash content (%) | 13.7 ± 0.1 | 19.7 ± 0.2 |
| Volatile matter (%) | 73.6 ± 0.1 | 65.4 ± 0.3 |
| Fixed carbon[c] (%) | 12.7 ± 0.1 | 14.9 ± 0.2 |
| HHV (MJ/kg) | 17.6 ± 0.1 | 21.6 ± 0.1 |

[a] Average values of three determinations with standard deviations.
[b] By difference
[c] 100 – (moisture + ash + volatile matter).

Table 3. Kinetic model checked to fit the experimental results of cumulative methane yield.

| Model | Equation | Parameters |
|---|---|---|
| First-order | $G(t) = G_{max}[1 - exp\,(-k \cdot t)]$ | *G* (mL $CH_4$/g COD): cumulative specific methane production<br>$G_{max}$ (mL $CH_4$/g COD): ultimate methane production<br>*k* ($d^{-1}$): specific rate constant<br>*t* (d): digestion time |
| Gompertz | $G(t) = G_{max} \cdot exp\,[-exp\,(\mu - \lambda \cdot t)]$ | *μ* (mL $CH_4$/g COD d): maximum methane production rate<br>*λ* (d): lag-phase time constant. |
| Modified Gompertz | $G(t) = G_{max} - exp\left[-exp\left(\frac{\mu}{G_{max}} \cdot (\lambda - t) \cdot e^1 + 1\right)\right]$ | $e^1$ = 2.7182 |
| Cone | $G(t) = \frac{G_{max}}{1 + (k \cdot t)^{-n}}$ | *n*: dimensionless shape factor |
| Weibull | $G(t) = G_{max} \cdot [1 - exp\,(-(k \cdot (\lambda - t))^d)]$ | *d*: dimensionless factor |

Table 4. Experimental maximum methane yield* ($G_{me}$) and fitting parameters for FS experiments.

| Model | Parameter | LFHTC to PSS mixture ratio (%) | | | | |
|---|---|---|---|---|---|---|
| | | **0** | **25** | **50** | **75** | **100** |
| Experimental | $G_{me}$ (mL $CH_4$/g COD) | 204 ± 1[a] | 172 ± 1[b] | 142 ± 4[c] | 124 ± 6[d] | 98 ± 3[e] |
| First-order | $G_m$ (mL $CH_4$/g COD) | 199 ± 4 | 166 ± 3 | 137 ± 3 | 120 ± 2 | 98 ± 2 |
| | $k$ ($d^{-1}$) | 0.160 ± 0.011 | 0.168 ± 0.012 | 0.162 ± 0.011 | 0.137 ± 0.009 | 0.100 ± 0.006 |
| | $R^2$ | 0.985 | 0.984 | 0.985 | 0.986 | 0.992 |
| | RCS | 74.7 | 54.1 | 35.2 | 24.2 | 9.3 |
| Gompertz | $G_m$ (mL $CH_4$/g COD) | 192 ± 4 | 161 ± 4 | 133 ± 3 | 117 ± 3 | 100 ± 4 |
| | $\mu$ (mL $CH_4$/g COD d) | 0.987 ± 0.156 | 0.935 ± 0.165 | 0.811 ± 0.160 | 0.757 ± 0.145 | 0.737 ± 0.116 |
| | $\lambda$ (d) | 0.315 ± 0.043 | 0.315 ± 0.047 | 0.271 ± 0.042 | 0.215 ± 0.032 | 0.141 ± 0.020 |
| | $R^2$ | 0.968 | 0.962 | 0.955 | 0.956 | 0.960 |
| | RCS | 125.0 | 100.6 | 78.9 | 61.6 | 38.9 |
| Modified Gompertz | $G_m$ (mL $CH_4$/g COD) | 71 ± 2 | 59 ± 1 | 50 ± 1 | 50 ± 3 | 50 ± 10 |
| | $\mu$ (mL $CH_4$/g COD d) | 8.181 ± 1.032 | 6.860 ± 0.948 | 4.616 ± 0.656 | 2.110 ± 0.399 | 1.045 ± 0.226 |
| | $\lambda$ (d) | 3.138 ± 0.271 | 2.965 ± 0.289 | 3.074 ± 0.371 | 4.458 ± 1.027 | 8.916 ± 4.338 |
| | $R^2$ | 0.968 | 0.962 | 0.953 | 0.893 | 0.835 |
| | RCS | 125.0 | 100.6 | 81.7 | 149.6 | 159.6 |
| Cone | $G_m$ (mL $CH_4$/g COD) | 204 ± 3 | 171 ± 3 | 144 ± 4 | 131 ± 4 | 111 ± 5 |
| | $k$ ($d^{-1}$) | 0.236 ± 0.010 | 0.246 ± 0.012 | 0.232 ± 0.014 | 0.185 ± 0.014 | 0.123 ± 0.012 |
| | n | 1.646 ± 0.107 | 1.591 ± 0.118 | 1.430 ± 0.116 | 1.293 ± 0.107 | 1.208 ± 0.091 |
| | $R^2$ | 0.995 | 0.993 | 0.992 | 0.992 | 0.994 |
| | RCS | 27.1 | 23.9 | 18.9 | 14.4 | 7.1 |
| Weibull | $G_m$ (mL $CH_4$/g COD) | 201 ± 3 | 169 ± 3 | 143 ± 3 | 128 ± 4 | 106 ± 4 |
| | $k$ ($d^{-1}$) | 0.926 ± 0.091 | 0.925 ± 0.082 | 0.929 ± 0.067 | 0.946 ± 0.055 | 0.938 ± 0.076 |
| | $\lambda$ (d) | 0.807 ± 0.061 | 0.761 ± 0.061 | 0.695 ± 0.053 | 0.677 ± 0.044 | 0.735 ± 0.043 |
| | $d$ | 0.200 ± 0.013 | 0.206 ± 0.015 | 0.185 ± 0.016 | 0.139 ± 0.013 | 0.095 ± 0.009 |
| | $R^2$ | 0.992 | 0.991 | 0.992 | 0.995 | 0.996 |
| | RCS | 31.2 | 23.8 | 13.8 | 7.6 | 3.7 |

*Average values of three determinations with standard deviations. Means with different superscript significant differ ($p < 0.05$).

RCS: Reduced Chi-Square.

Table 5. Experimental maximum methane yield* ($G_{me}$) and fitting parameters for GS experiments.

| Model | Parameter | LFHTC to PSS mixture ratio (%) | | | | |
|---|---|---|---|---|---|---|
| | | **0** | **25** | **50** | **75** | **100** |
| Experimental | $G_{me}$ (mL $CH_4$/g COD) | 308 ± 1[a] | 248 ± 11[b] | 224 ± 11[b,c] | 204 ± 9[c,d] | 191 ± 1[d] |
| First-order | $G_m$ (mL $CH_4$/g COD) | 328 ± 18 | 249 ± 8 | 221 ± 6 | 199 ± 4 | 186 ± 3 |
| | $k$ ($d^{-1}$) | 0.059 ± 0.007 | 0.066 ± 0.005 | 0.068 ± 0.004 | 0.068 ± 0.003 | 0.060 ± 0.002 |
| | $R^2$ | 0.979 | 0.990 | 0.994 | 0.996 | 0.998 |
| | RCS | 251.2 | 68.2 | 34.5 | 17.4 | 7.7 |
| Gompertz | $G_m$ (mL $CH_4$/g COD) | 292 ± 5 | 232 ± 4 | 209 ± 4 | 191 ± 4 | 181 ± 5 |
| | $\mu$ (mL $CH_4$/g COD d) | 1.179 ± 0.084 | 1.007 ± 0.078 | 0.947 ± 0.083 | 0.897 ± 0.084 | 0.820 ± 0.078 |
| | $\lambda$ (d) | 0.147 ± 0.010 | 0.135 ± 0.010 | 0.130 ± 0.011 | 0.122 ± 0.011 | 0.098 ± 0.009 |
| | $R^2$ | 0.990 | 0.988 | 0.985 | 0.983 | 0.981 |
| | RCS | 110.6 | 78.6 | 78.8 | 73.0 | 68.3 |
| Modified Gompertz | $G_m$ (mL $CH_4$/g COD) | 107± 2 | 85 ± 2 | 77 ± 2 | 70 ± 2 | 67 ± 2 |
| | $\mu$ (mL $CH_4$/g COD d) | 5.804 ± 0.345 | 4.235 ± 0.266 | 3.676 ± 0.257 | 3.149 ± 0.233 | 2.415 ± 0.18 |
| | $\lambda$ (d) | 8.016 ± 0.327 | 7.471 ± 0.364 | 7.291 ± 0.415 | 7.351 ± 0.462 | 8.33 2 ± 0.583 |
| | $R^2$ | 0.990 | 0.988 | 0.985 | 0.983 | 0.981 |
| | RCS | 110.6 | 78.6 | 78.8 | 73.0 | 68.3 |
| Cone | $G_m$ (mL $CH_4$/g COD) | 300 ± 16 | 264 ± 7 | 242 ± 5 | 226 ± 5 | 235 ± 6 |
| | $k$ ($d^{-1}$) | 0.091 ± 0.008 | 0.090 ± 0.005 | 0.088 ± 0.004 | 0.083 ± 0.004 | 0.060 ± 0.003 |
| | n | 1.793 ± 0.249 | 1.487 ± 0.085 | 1.382 ± 0.062 | 1.290 ± 0.047 | 1.108 ± 0.033 |
| | $R^2$ | 0.976 | 0.995 | 0.997 | 0.998 | 0.999 |
| | RCS | 284.1 | 33.4 | 16.3 | 8.7 | 4.2 |
| Weibull | $G_m$ (mL $CH_4$/g COD) | 297 ± 7 | 242 ± 6 | 222 ± 5 | 205 ± 5 | 206 ± 5 |
| | $k$ ($d^{-1}$) | 0.119 ± 0.949 | 0.269 ± 0.599 | 0.514 ± 0.402 | 0.641 ± 0.273 | 0.686 ± 0.149 |
| | $\lambda$ (d) | 1.321 ± 0.183 | 1.1 ± 0.115 | 0.992 ± 0.083 | 0.922 ± 0.059 | 0.833 ± 0.033 |
| | $d$ | 0.073 ± 0.006 | 0.072 ± 0.004 | 0.071 ± 0.004 | 0.067 ± 0.004 | 0.051 ± 0.003 |
| | $R^2$ | 0.990 | 0.992 | 0.994 | 0.996 | 0.999 |
| | RCS | 119.8 | 51.2 | 30.3 | 16.2 | 4.8 |

*Average values of three determinations with standard deviations. Means with different superscript significant differ ($p < 0.05$).

RCS: Reduced Chi-Square.

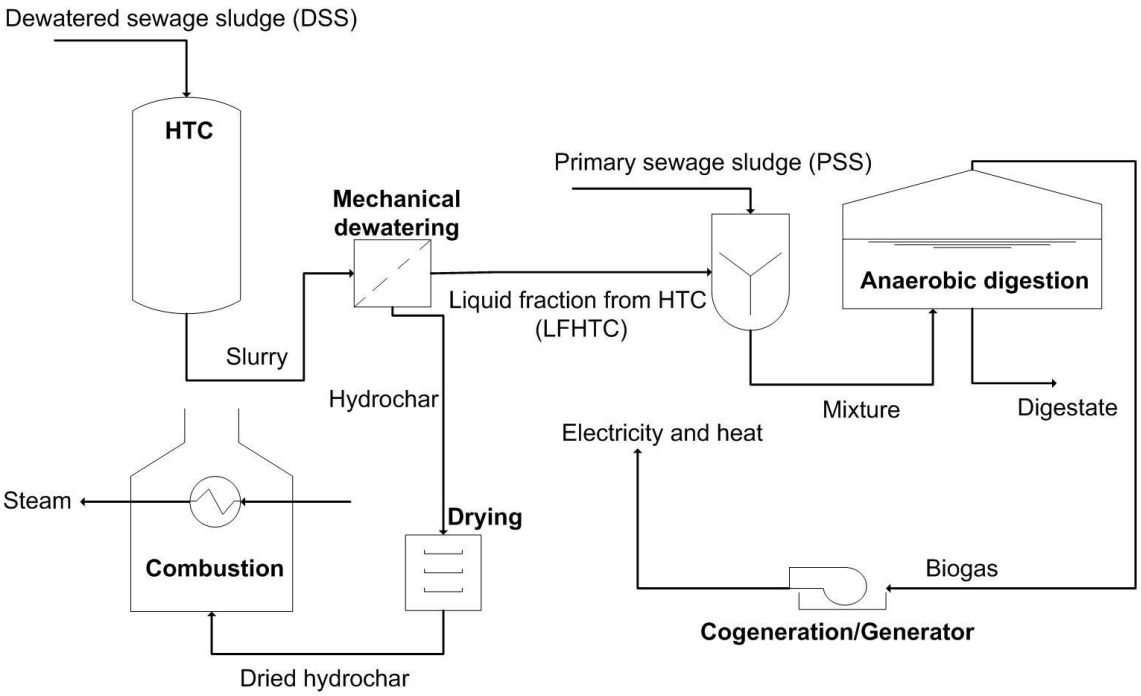


Fig. 1. Integration of HTC of dewatered waste activated sludge into the scheme of sludge processing in a WWTP.

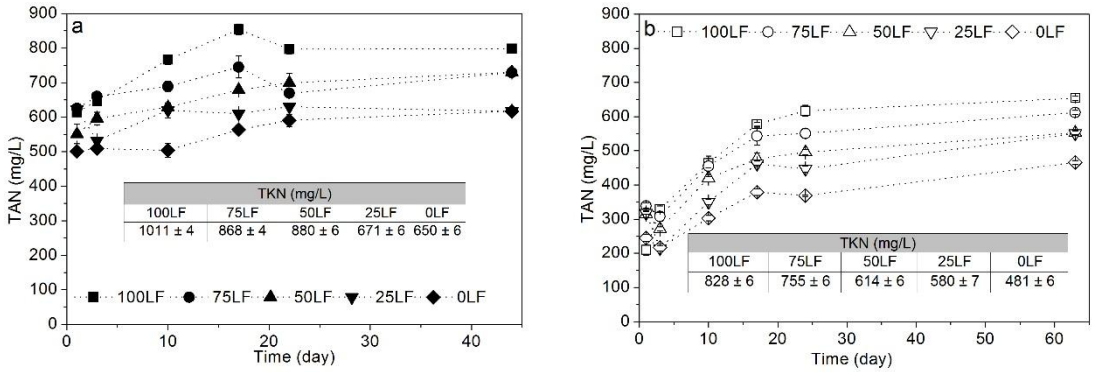


Fig. 2. Time-course of total ammonia nitrogen (TAN) along the anaerobic co-digestion of PSS and LFHTC with FS (a) and GS (b) inocula. Tables show the TKN values.

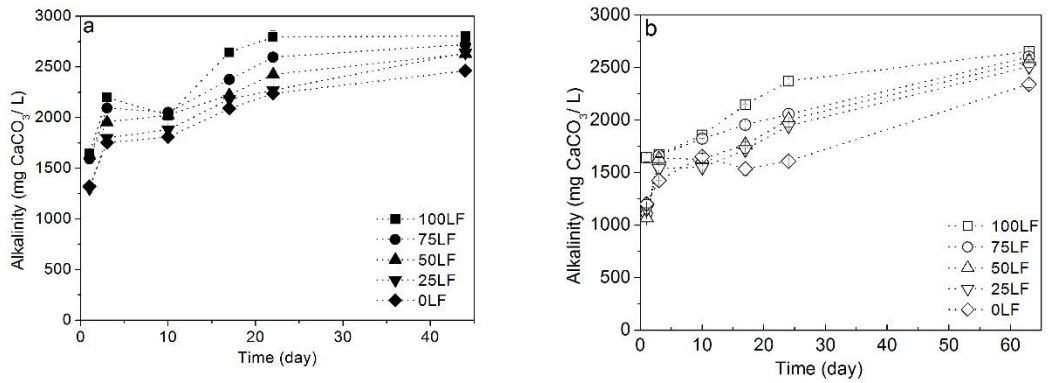


Fig. 3. Time-course of total alkalinity along the anaerobic co-digestion of PSS and LFHTC with FS (a) and GS (b) inocula.

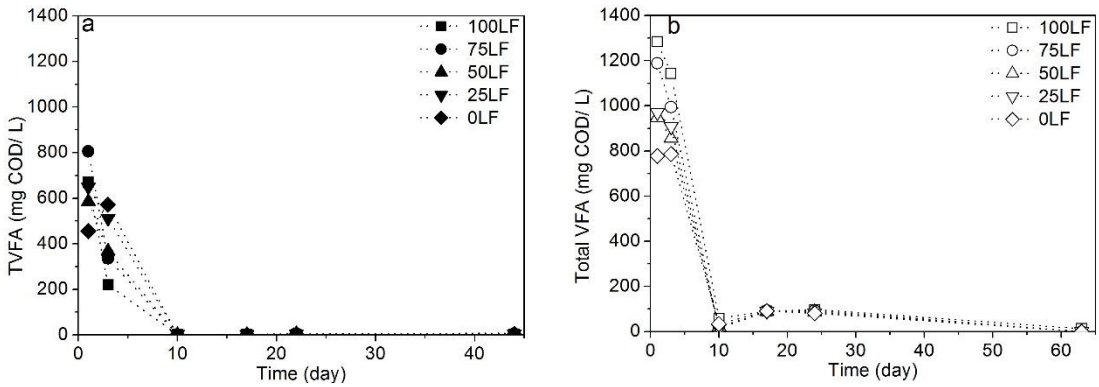


Fig. 4. Time-course of total VFA along the anaerobic co-digestion of PSS and LFHTC with FS (a) and GS (b) inocula.

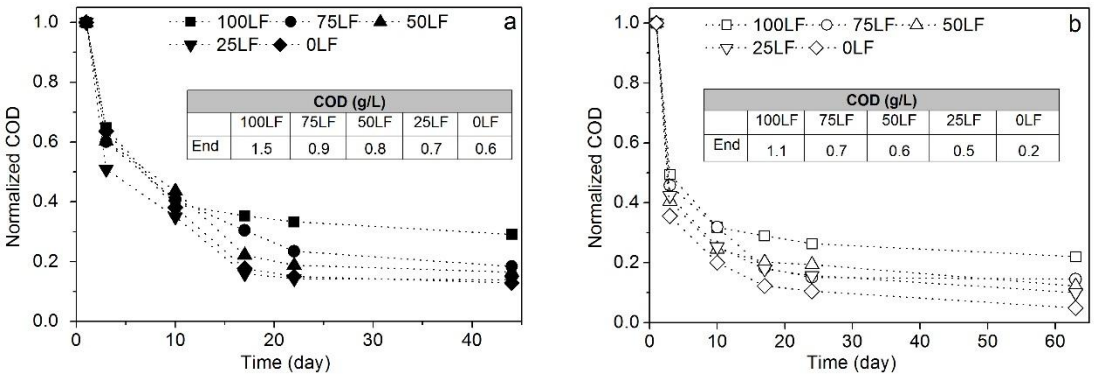


Fig. 5. Time-course of soluble COD along the anaerobic co-digestion of PSS and LFHTC with FS (a) and GS (b) inocula.

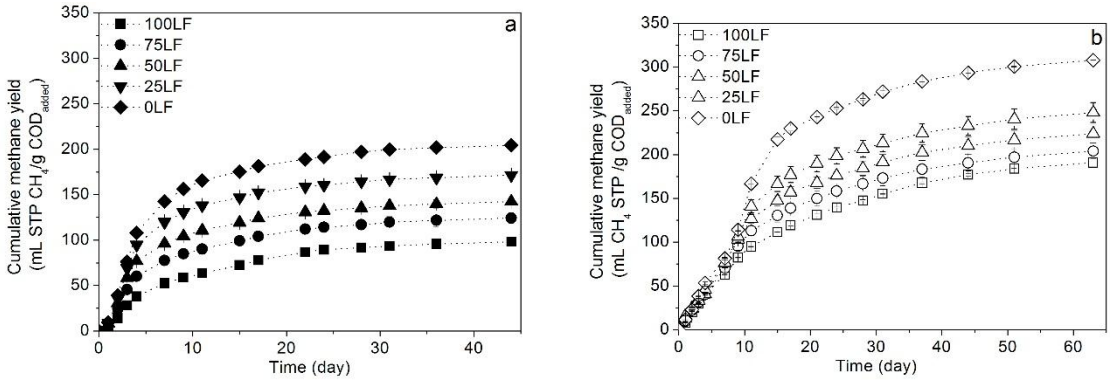


Fig. 6. Cumulative methane yield along the anaerobic co-digestion of PSS and LFHTC with FS (a) and GS (b) inocula.

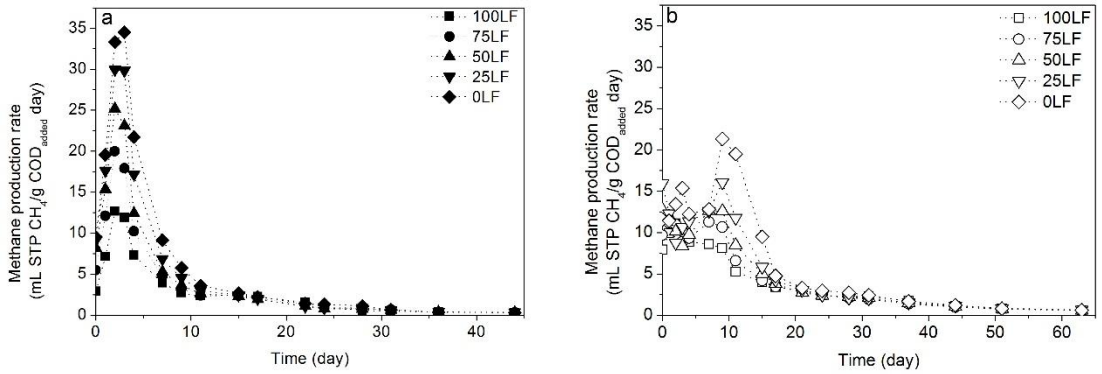


Fig. 7. Time-course of daily methane production rate along the anaerobic co-digestion of PSS and LFHTC with FS (c) and GS (d) inocula.